RESEARCH ARTICLE | DECEMBER 02 2021

Optical pump assisted broadband terahertz frequency comb

Special Collection: 2021 Photonics and Optics

Kai Wang; Ning Yang ; Peng Bai ; Weidong Chu ; Yuanyuan Li ; Jian Wang

AIP Advances 11, 125101 (2021)
https://doi.org/10.1063/5.0071846

Optical pump assisted broadband terahertz frequency comb

Cite as: AIP Advances 11, 125101 (2021); doi: 10.1063/5.0071846
Submitted: 17 September 2021 • Accepted: 5 November 2021 •
Published Online: 2 December 2021

Kai Wang,[1] Ning Yang,[1,a)] Peng Bai,[1] Weidong Chu,[1] Yuanyuan Li,[2,3] and Jian Wang[4]

AFFILIATIONS

[1] Institute of Applied Physics and Computational Mathematics, Beijing 100088, China
[2] Institute of Microelectronics, Tsinghua University, Beijing 100084, China
[3] Beijing National Research Center for Information Science and Technology (BNRist), Tsinghua University, Beijing 100084, China
[4] Department of Physics, Beijing Jiaotong University, Beijing 100044, China

[a)] **Author to whom correspondence should be addressed:** yang_ning@iapcm.ac.cn

ABSTRACT

A broadband terahertz (THz) frequency comb assisted by an optical pump in THz quantum cascade lasers (QCLs) is investigated theoretically and numerically through a Maxwell–Bloch model combined with the coupled wave theory. When an optical pump is injected into the laser cavity with dispersion, the intrinsic four-wave-mixing nonlinear process becomes not only an important elementary phase-locking mechanism during the mode proliferating process, but also the bandwidth of the frequency comb is increased and the power is amplified through the nonlinear parametric process. The relative shift between the frequency of the optical pump and the zero-dispersion frequency of THz QCLs tremendously affects the conversion efficiency of the nonlinear parametric process. The simulation results show that appropriately optical pumping could assist in generating the broadband THz frequency comb with over 1 THz and more than 80 lines, which may open many potential applications in designing and optimizing high resolution THz spectroscopy sources.

I. INTRODUCTION

Composed of numerous highly coherent and equally spaced laser longitudinal modes, optical frequency combs[1–6] have many unique features, such as ultrahigh frequency stability and ultralow phase noise, which make them potential candidates for large capacity radio-frequency communication,[7] sensor imaging,[8] and spectral metrology.[9–11] In particular, since many molecules' characteristic absorption spectral lines lie in the THz spectral range,[12] highly accurate material detection has come into reality by detecting the absorption of comb lines through dual-comb spectroscopy technology.[13] There are several actively and positively mode-locked methods to produce THz frequency combs in THz quantum cascade lasers (QCLs), including the microwave modulating the laser current[14,15] and a graphene-coupled saturable absorber.[16] Compared with the optical frequency combs traditionally generated by a mode-locked laser,[17] THz QCLs are capable of generating THz frequency combs through the four-wave-mixing (FWM) nonlinear effect,[18] which shows constant instantaneous power instead of a short pulse in the time domain and similar frequency modulated signals, due to very fast gain recovery[19] in QCLs. Unfortunately, it is very difficult to generate many high-power modes only by using an electrical pump in THz QCLs due to orders of magnitude higher dispersion. Although dispersion compensation methods[20,21] have been proposed, it is almost impossible to reduce this dispersion to the level of mid-infrared QCLs. Furthermore, only the correctly compensated THz QCLs could generate combs effectively.

The optically pumped nonlinear parametric process originates from the highest third-order nonlinear susceptibility in optical waveguides, such as high nonlinear optical fibers[22–26] and silicon nanophotonic waveguides.[27–31] The active region of QCLs intrinsically shows much higher nonlinearity. A very large value of the third-order nonlinearity susceptibility has been measured experimentally, and obvious degenerate nonlinear parametric process has also been observed.[32] Based on the high nonlinearity in QCLs and dispersion engineering, this parametric process enables amplification, and at the same time, the comb lines can also be symmetrically duplicated on the other side of the pump when phase-matching condition is achieved. Therefore, it could provide a wide frequency comb bandwidth in mid-infrared QCLs through phase-matching

controlling.[33] However, such a phase-matching method may be difficult to be applied to THz QCLs because of the complex dispersion profile of the laser active region. Optical parametric process with high conversion efficiency usually requires the pump frequency to be near the zero-dispersion frequency, to meet the momentum conservation condition in the nonlinear process of FWM. Nevertheless, with the assistance of waveguide engineering, for example, a chirped corrugated mirror is integrated into the QCL waveguide to make the longer-wavelength wave travel further,[20] the position of the zero-dispersion frequency in the frequency domain of a THz QCL can be controlled artificially,[34] and then the broadband frequency comb can be effectively excited by optical pumping.

To achieve broadband frequency combs in THz QCLs, the optically pumped parametric process may play an interesting and significant role. In this work, we fully utilize the time evolution simulations of the THz QCLs comb based on a Maxwell–Bloch model to represent the dynamics of the comb modes and an optically assisted pump whose frequency locates near the zero-dispersion frequency of the waveguide to investigate the possibility of broadening the bandwidth of the THz-QCLs comb.

II. MODEL AND METHODS

The schematic diagram of an optical pump assisted broadband frequency comb is illustrated in Fig. 1. In order to model the optical pump assisted THz frequency comb, we employ the optical Bloch equations to describe the dynamics of a THz QCLs frequency comb in the model of a two-level system, including the population interaction as well as coherences between the upper and ground states. Then, the Maxwell equation is utilized to establish the electromagnetic interaction between the frequency comb and a high-power single optical pump in the active laser cavity.

To model the THz QCLs frequency comb, Khurgin *et al.*[35] and Villares and Faist[36] theoretically proposed and developed self-frequency-modulated Maxwell–Bloch formalism by taking the assumption that the ground state population is negligible and three order perturbative approximation. Following similar methods and symbols, the final coupled equations that describe the time evolution of the complex amplitude of the slowly varying envelope of the optical fields of all comb modes and the optical pump are

$$\frac{dA_n}{dT} = (G_n - 1 + iD_n)A_n - G_n\sum_{k,l=-\frac{N}{2}}^{\frac{N}{2}} A_m A_k A_l^* B_{kl} C_{kl}\kappa_{klmn}, \quad (1)$$

where the complex envelope A_n of mode n is normalized to the saturation field $A_{sat} = \hbar/u_{21}\sqrt{(\tau_{coh}\tau_2)}$, τ_{coh} represents the coherent time of the laser transition (which is the relaxation time between the intersubband transition states), τ_2 is the lifetime of the upper state, and u_{21} is the dipole matrix element between the upper and lower radiation states. The first term on the right-hand side of the equation describes the gain and dispersion, and the second term represents the FWM nonlinear process. Furthermore, the parametric process also generates idler modes through the summation term. Note that we do not consider the pump consumption here.

The subscripts in the second term of Eq. (1) satisfy the relationship $n + l = m + k$, which represents the relationship of four-wave mixing terms, and a dimensionless time T is introduced to normalize the real time to the photon lifetime by $T = t/2t_c$. The gain for the mode n is written by

$$G_n = g_0\left[1 + n^2\left(\frac{\tau_{coh}}{\tau_{rt}}\right)^2\right]^{-1}, \quad (2)$$

where g_0 is the gain of the intersubband transition, which is normalized to the lasing threshold, $g_0 = \omega_0\tau_c N u_{21}^2\Delta\rho_p/2\varepsilon_0 n_0^2\hbar$. The round-trip time of the l_c length cavity is $\tau_{rt} = 2l_c n_g/c$, where n_0 is the refractive index, n_g is the group index, and c is the velocity of speed. The dispersion term can be written by[35]

$$D_n = \frac{\omega_n^2 - \omega_{nc}^2}{2\omega_n}, \quad (3)$$

where ω_n is the frequency of the nth mode with $\omega_n = \omega_{21} + n\omega$ (where ω_{21} is the central resonant frequency of the laser transition and the mode spacing $\omega = 2\pi/\tau_{rt}$) and the empty cavity frequency $\omega_{nc} = \omega_{21} + \Delta\omega$ (where the frequency shift is $\Delta\omega = n\pi c(2n_g^2 l_c - n\pi c^2\beta_2)/2n_g^3 l_c^2$ and the group velocity dispersion parameter is $\beta_2 = d^2k/d\omega^2$). The FWM coefficients B_{kl} and C_{kl} are given by

$$B_{kl} = \left[1 + \frac{1}{2}(k^2 + l^2)\left(\frac{\tau_{coh}}{\tau_{rt}}\right)^2\right]^{-1}, \quad (4)$$

$$C_{kl} = \left[1 - \frac{1}{2}i(k - l)\left(\frac{\tau_2}{\tau_{rt}}\right)\right]^{-1}. \quad (5)$$

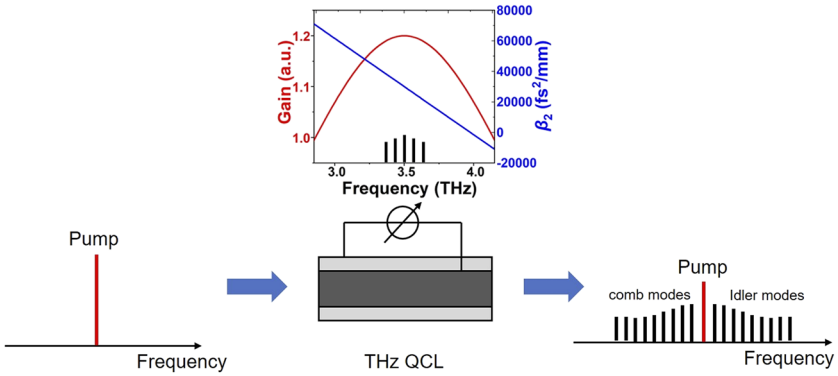

FIG. 1. Schematic diagram of the optical pump assisted broadband THz QCLs frequency comb. The inset shows the gain and dispersion parameter β_2 of the THz QCLs.

TABLE I. Typical values in the simulations.

Parameter	Symbol	Typical value	References
The photon lifetime in the QCLs' cavity	τ_c	21 ps	35
The inter-subband transition coherent time of QCLs	τ_{coh}	0.7 ps	35
The lifetime of the upper state	τ_2	12 ps	36
The refractive index	n_0	3.6	34
The dipole matrix element	u_{21}	4.0 nm × e	34
The saturation field	A_{sat}	5.66×10^4 V/m	
The length of the laser cavity	L	3 mm	
The velocity of speed	c	3×10^8 m/s	
The unsaturated gain (normalized to the laser threshold)	g_0	1.2	

Meanwhile, the intermodal overlap factor κ_{klmn} is as follows:

$$\kappa_{klmn} = \frac{1}{l_c}\int_0^{l_c} \sin(k_k x)\sin(k_l x)\sin(k_m x)\sin(k_n x). \quad (6)$$

Since there is one high power optical pump, the same FWM mechanism can induce high degenerate parametric amplification and wavelength conversion simultaneously, where optical gain and idler modes occur. Except for the optical pump, the initial conditions of Eq. (1) are set by the same small field amplitude and random phases that represent typical THz QCLs. In the simulations, in order to reduce the simulation time and the computational load, several simplifications are adopted, such as the limited number of modes, and the frequencies of the optical pump and zero-dispersion are artificially set exactly on the comb modes. All the parameters and typical values of the THz QCLs are listed in Table I.

III. RESULTS AND DISCUSSIONS

First, we show the dynamics of the THz frequency combs with and without the optical pump. Note that the gain center of the THz QCLs is always set at 3.5 THz and the zero-dispersion frequency is offset by 30 modes (about 3.977 THz), which is always set at mode 0 in all the following simulations. The simulation results of output

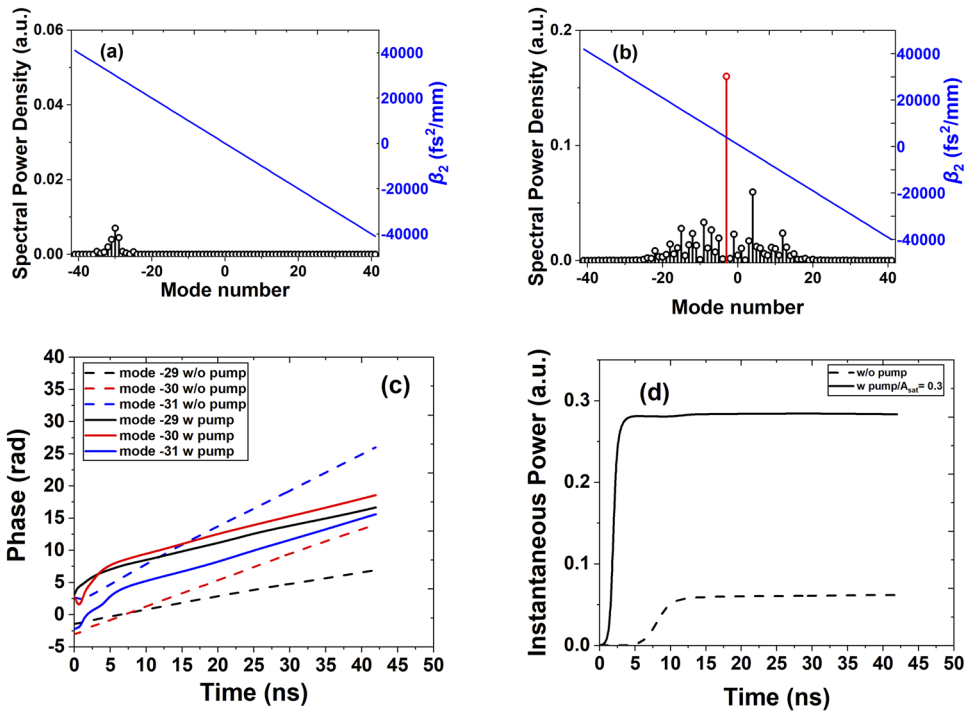

FIG. 2. Simulations of the THz frequency comb with and without the optical pump. Spectral power density (a) without the optical pump and (b) with the optical pump. (c) The phase evolution of the mode −29, −30, and −31 with and without the optical pump. (d) Time dependent optical instantaneous power of the frequency comb with and without optical pump.

spectral power density, phase, and instantaneous power evolution are depicted in Fig. 2. As shown in Fig. 2(a), the power density spectrum of the THz frequency comb without the optical pump injected is composed of only less than 8 mode lines with very low power. This is because the gain center is far from the zero-dispersion frequency; thus, the dispersion is very large and no appropriate dispersion can be obtained by dispersion compensation as well. When an optical pump with the power of $0.3A_{sat}$ and frequency at mode −3 is employed, the power density spectrum is shown in Fig. 2(b). The optical pump not only amplifies the original frequency comb but also replicates the frequency comb, and as a result, the number of the frequency comb modes is increased to more than 50. Figure 2(c) shows the phase evolution of the modes −29, −30, and −31 with and without the optical pump, respectively. The slope of the phase evolution is due to the dispersion effect, and the magnitude of the slope represents the degree that the real mode frequency deviates from the equally spaced frequency without dispersion.[34] This frequency offset can be calculated directly by the following equation: $d\omega = d(\arg(A_n))/dt$. Compared with the self-referencing phase-locked process without the optical pump that the values of frequency offset of mode −29, −30, and −31 are 0.2815, 0.3741, and 0.5656 GHz, respectively, the slope of the phase is suppressed to 0.2533, 0.2824, and 0.3350 GHz, which indicates that the modes are locked better. Meanwhile, the time of phase stabilization is slightly increased by introducing the single optical pump, from less than 5 ns to more than 10 ns. In the time domain, the instantaneous power eventually tends to be constant when the steady state is reached, and with the optical pump injected, the time to reach constant power output is significantly reduced compared with the case where no optical pump is employed, as shown in Fig. 2(d).

In order to study and optimize the bandwidth of the THz frequency comb, we first studied the impact of the pump frequency. As seen from Figs. 3(a) and 3(c), within a certain frequency range, the pump frequency close to the zero-dispersion frequency can increase the bandwidth of the THz frequency comb where zero-dispersion frequency is set at mode 0, note that we have set the field of the optical pump to be $0.4A_{sat}$. When the pump frequency is detuned from the zero-dispersion frequency by repetition frequency ω, the number of comb lines increases to more than 80, which is one order of magnitude more than that without pump injection [Fig. 2(a)]. In Fig. 3(d), we show the phase evolution of mode −30 when the frequency offset of the optical pump relative to the zero-dispersion frequency is ω, 3ω, and 5ω, respectively. The closer the pump frequency is to the zero-dispersion frequency, the smaller the slope of the phase, indicating that the phase mismatch is suppressed, so that more optical power is converted; thus, the bandwidth of the

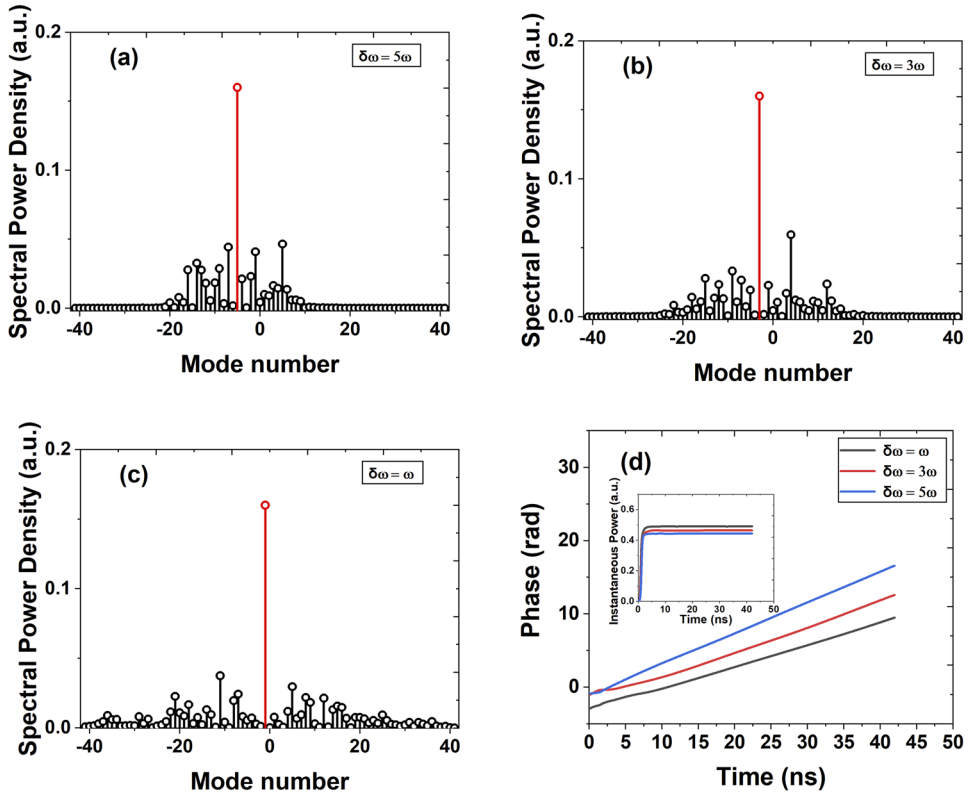

FIG. 3. Simulation results of the effect of pump frequency on the optical frequency comb. Spectral power density with (a) pump offset = 5ω, (b) pump offset = 3ω, and (c) pump offset = 1ω. (d) The phase evolution of mode −30 when the frequency offset of the optical pump relative to the zero-dispersion frequency is ω, 3ω, and 5ω, respectively. The inset shows the time dependent optical instantaneous power of the frequency comb with pump offset = ω, 3ω, and 5ω, respectively.

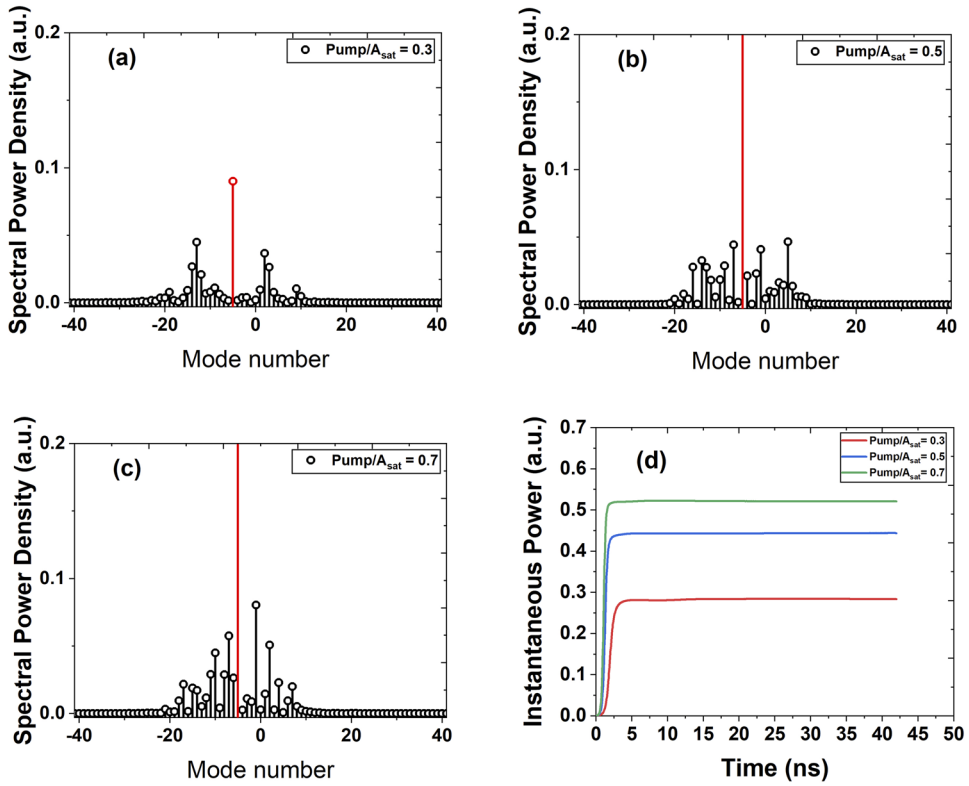

FIG. 4. Simulation results of the effect of pump power on the optical frequency comb. Optical spectral power density with (a) pump/A_{sat} = 0.3, (b) pump/A_{sat} = 0.5, and (c) pump/A_{sat} = 0.7. (d) Time dependent optical instantaneous power with pump/A_{sat} = 0.3, 0.5, and 0.7, respectively.

frequency comb is effectively increased. In addition, from the time evolution of the instantaneous power shown in the inset of Fig. 3(d), it can be seen that the pump frequency has no effect on the evolution time when the THz QCLs comb reaches steady state, but only has a slight effect on the power of the comb.

Then, we investigate the effect of pump power on the instantaneous power and optical power spectral density of the THz frequency comb, as shown in Fig. 4. It is obvious that the higher the optical pump power, the stronger the power output of the frequency comb, but the bandwidth of the frequency comb is not expanded very much. It should be noted, however, that the power of the comb lines within the bandwidth is enhanced by a higher optical pump. In addition, by raising the injected optical pump power, we can reduce the time for the frequency comb to enter the steady state, as depicted in Fig. 4(d). Eventually, the constant power output of the THz frequency combs is achieved.

IV. CONCLUSION

In conclusion, based on the numerical solution of the Maxwell–Bloch model and the coupled wave theory in the slowly varying envelope and a three order perturbative approximation, we have presented the dynamics of broadband THz frequency combs by introducing an assisted optical pump, taking into account the dispersion. FWM enables both the self-reference phase locking and nonlinear parametric process. We have shown that, with the optical pump injected, the number of the comb lines is more than 80 by setting the frequency of the optical pump close to the zero-dispersion frequency, resulting in a much broader frequency comb. This optical pump nonlinear parametric process could be very promising. On the one hand, a single pump parametric scheme can be simply equipped. On the other hand, not only could the newly generated idler modes during the parametric amplification process double the number of the optical frequency comb, but also carry the phase information conjugate with the original comb modes. Moreover, very low phase noise in the nonlinear parametric process can keep the frequency comb in good coherence, which is our future research. All these can enhance the detection ability of the QCLs THz frequency comb and, therefore, lead to a growing number of spectroscopic applications.

ACKNOWLEDGMENTS

This work was funded by the National Natural Science Foundation of China (NSAF) (Grant No. U1730246).

AUTHOR DECLARATIONS

Conflict of Interest

The authors have no conflicts to disclose.

DATA AVAILABILITY

The data that support the findings of this study are available from the corresponding author upon reasonable request.

REFERENCES

[1] L. Consolino, M. Nafa, F. Cappelli, K. Garrasi, F. P. Mezzapesa, L. Li, A. G. Davies, E. H. Linfield, M. S. Vitiello, P. De Natale, and S. Bartalini, Nat. Commun. **10**, 2938 (2019).
[2] A. Schliesser, N. Picqué, and T. W. Hänsch, Nat. Photonics **6**, 440 (2012).
[3] A. Hugi, G. Villares, S. Blaser, H. C. Liu, and J. Faist, Nature **492**, 229 (2012).
[4] S. A. Diddams, J. Opt. Soc. Am. B **27**, B52 (2010).
[5] D. Kazakov, M. Piccardo, Y. Wang, P. Chevalier, T. S. Mansuripur, F. Xie, C.-e. Zah, K. Lascola, A. Belyanin, and F. Capasso, Nat. Photonics **11**, 789 (2017).
[6] G. Scalari, J. Faist, and N. Picqué, Appl. Phys. Lett. **114**, 150401 (2019).
[7] A. L. Gaeta, M. Lipson, and T. J. Kippenberg, Nat. Photonics **13**, 158 (2019).
[8] Y. Li, N. Yang, Y. Xie, W. Chu, W. Zhang, S. Duan, and J. Wang, Opt. Express **27**, 3146 (2019).
[9] T. Udem, R. Holzwarth, and T. W. Hänsch, Nature **416**, 233 (2002).
[10] N. Leindecker, A. Marandi, R. L. Byer, K. L. Vodopyanov, J. Jiang, I. Hartl, M. Fermann, and P. G. Schunemann, Opt. Express **20**, 7046 (2012).
[11] F. Keilmann, C. Gohle, and R. Holzwarth, Opt. Lett. **29**, 1542 (2004).
[12] L. Ge, N. Yang, J. Wang, Y. Li, W. Chu, S. Duan, and Y. Xie, Appl. Phys. Lett. **115**, 261105 (2019).
[13] G. Villares, A. Hugi, S. Blaser, and J. Faist, Nat. Commun. **5**, 5192 (2014).
[14] H. Li, P. Laffaille, D. Gacemi, M. Apfel, C. Sirtori, J. Leonardon, G. Santarelli, M. Rösch, G. Scalari, M. Beck, J. Faist, W. Hänsel, R. Holzwarth, and S. Barbieri, Opt. Express **23**, 33270 (2015).
[15] S. Barbieri, P. Gellie, G. Santarelli, L. Ding, W. Maineult, C. Sirtori, R. Colombelli, H. Beere, and D. Ritchie, Nat. Photonics **4**, 636 (2010).
[16] H. Li, M. Yan, W. Wan, T. Zhou, K. Zhou, Z. Li, J. Cao, Q. Yu, K. Zhang, M. Li, J. Nan, B. He, and H. Zeng, Adv. Sci. **6**, 1900460 (2019).
[17] H. A. Haus, IEEE J. Quantum Electron. **6**, 1173 (2000).
[18] J. Faist, G. Villares, G. Scalari, M. Rösch, C. Bonzon, A. Hugi, and M. Beck, Nanophotonics **5**, 271 (2016).
[19] M. C. Tatham, J. F. Ryan, and C. T. Foxon, Phys. Rev. Lett. **63**, 1637 (1989).
[20] D. Burghoff, T.-Y. Kao, N. Han, C. W. I. Chan, X. Cai, Y. Yang, D. J. Hayton, J.-R. Gao, J. L. Reno, and Q. Hu, Nat. Photonics **8**, 462 (2014).
[21] M. Rösch, G. Scalari, M. Beck, and J. Faist, Nat. Photonics **9**, 42 (2014).
[22] R. H. Stolen, J. E. Bjorkholm, and A. Ashkin, Appl. Phys. Lett. **24**, 308 (1974).
[23] J. Hansryd, P. A. Andrekson, M. Westlund, J. Li, and P.-O. Hedekvist, IEEE J. Sel. Top. Quantum Electron. **8**, 506 (2002).
[24] X. Liu, S. Chandrasekhar, P. J. Winzer, R. W. Tkach, and A. R. Chraplyvy, J. Lightwave Technol. **32**, 766 (2014).
[25] S. L. I. Olsson, B. Corcoran, C. Lundström, T. A. Eriksson, M. Karlsson, and P. A. Andrekson, J. Lightwave Technol. **33**, 710 (2015).
[26] K. Vijayan, Z. He, B. Foo, M. Karlsson, and P. A. Andrekson, Opt. Express **28**, 34623 (2020).
[27] T. J. Kippenberg, S. M. Spillane, and K. J. Vahala, Phys. Rev. Lett. **93**, 083904 (2004).
[28] P. Del'Haye, A. Schliesser, O. Arcizet, T. Wilken, R. Holzwarth, and T. J. Kippenberg, Nature **450**, 1214 (2007).
[29] X. Liu, R. M. Osgood, Jr., Y. A. Vlasov, and W. M. J. Green, Nat. Photonics **4**, 557 (2010).
[30] Y. Okawachi, K. Saha, J. S. Levy, Y. H. Wen, M. Lipson, and A. L. Gaeta, Opt. Lett. **36**, 3398 (2011).
[31] P. Trocha, M. Karpov, D. Ganin, M. H. P. Pfeiffer, A. Kordts, S. Wolf, J. Krockenberger, P. Marin-Palomo, C. Weimann, S. Randel, W. Freude, T. J. Kippenberg, and C. Koos, Science **359**, 887 (2018).
[32] D. Walrod, S. Y. Auyang, P. A. Wolff, and M. Sugimoto, Appl. Phys. Lett. **59**, 2932 (1991).
[33] P. Friedli, H. Sigg, B. Hinkov, A. Hugi, S. Riedi, M. Beck, and J. Faist, Appl. Phys. Lett. **102**, 222104 (2013).
[34] P. Tzenov, D. Burghoff, Q. Hu, and C. Jirauschek, Opt. Express **24**, 23232 (2016).
[35] J. B. Khurgin, Y. Dikmelik, A. Hugi, and J. Faist, Appl. Phys. Lett. **104**, 081118 (2014).
[36] G. Villares and J. Faist, Opt. Express **23**, 1651 (2015).